

# Optical surface waves at the interface between a linear dielectric and a photorefractive crystal

V A Aleshkevich, V A Vysloukh, Ya V Kartashov

**Abstract.** The propagation of a laser beam near the interface between a linear dielectric and a photorefractive crystal is considered. The specific features of formation of surface waves are studied, the profiles of such surface modes are numerically calculated, and guiding properties of the interface are analysed. Using the method of effective particles, the second-order ordinary differential equation describing the trajectory of a beam reflecting from the interface is obtained and analysed.

## 1. Introduction

The propagation of a laser beam near the interface between two media with different optical properties is a classical problem, which is important both from the theoretical and practical points of view. In this respect, of special interest are nonlinear interfaces when at least one of the media is nonlinear. During the propagation of a laser beam near such an interface, a surface wave can appear, the beam filamentation or fanning can occur, etc.

The features of the interaction of a laser beam with the interface between two media strongly depend on the type of nonlinearity of the latter. The interfaces of Kerr materials (including the linear-nonlinear [1, 2] and nonlinear-nonlinear [3] interfaces), materials with quadratic nonlinearity [4], as well as the interface between a Kerr medium and an absorbing medium [5] were earlier studied in many papers.

However, of prime interest for practical purposes is a study of the interaction of laser radiation with interfaces between media having more complicated nonlinearities. Considerable achievements [6, 7] in the generation of solitons in photorefractive crystals (PRCs), which possess nonlinear properties at rather low radiation intensities, stimulated studies of the features of formation of surface waves in photorefractive media.

The authors [8] considered the possibility of excitation of a surface wave near the interface between a PRC having purely diffusion nonlinearity and a linear medium (dielectric or metal). They showed that the energy of such a wave could concentrate within a thin surface layer of a PRC. In this case,

the surface wave appears due the interference and energy exchange between the waves reflected from the interface and a Bragg grating formed inside the crystal. Later [9, 10], the near-surface propagation of a laser beam in the presence of the drift and diffusion components of the nonlinear response of a PRC was interpreted as a result of the balance of the beam self-bending, caused by the presence of the diffusion component of the nonlinear response of a PRC, and reflection [11].

One of the important features of the near-surface propagation of a laser beam is that the energy concentration within a thin layer of a substance considerably reduces the characteristic response time of a PRC. This allows one to increase substantially the operation rate of optical devices based on photorefractive materials without the use of additional waveguide optical structures [12, 13]. The use of the competition between the beam self-bending and reflection of radiation from the interface permits the construction of waveguide structures, which play the role of logical elements and devices for controlling light by light.

Although photorefractive surface waves have been studied in many papers, this problem is not adequately studied so far. In fact, the authors of the most of earlier papers [8–10] studied surface waves in PRCs that had a specific logarithmic nonlinearity, which allowed one to obtain linearised equations for the envelope of a surface wave in the case of a low dark conductivity of the PRC.

In this paper, we consider the interaction of a laser beam with the interface between a linear dielectric and a PRC with a sufficiently high dark conductivity. We took into account both the drift and diffusion component of a nonlinear response. This means that we considered the addition to the refractive index, which is proportional to the first derivative of the incident radiation intensity and results in the beam self-bending [14]. An analytic treatment of the beam trajectory is based on the method of effective particles, which is well known in quantum mechanics (the detailed description of the method is presented in paper [3]). In addition, we calculated numerically exact profiles of surface modes.

## 2. Theoretical model

Consider the propagation of a slit (infinite along the  $y$ -axis and finite along the  $x$ -axis) beam along the  $z$ -axis near the interface between a linear dielectric occupying the half-space  $x \geq 0$  and a PRC occupying the half-space  $x < 0$ . We assume that the beam is polarised along the  $y$ -axis. The propagation of the beam is described by the standard truncated wave equation for the normalised complex amplitude  $q(\eta, \xi)$  of the field

---

V A Aleshkevich, V A Vysloukh, Yu V Kartashov International Teaching and Research Laser Centre, M V Lomonosov Moscow State University, Vorob'evy gory, 119899 Moscow, Russia

Received 17 March 2000

*Kvantovaya Elektronika* 30 (10) 905–910 (2000)

Translated by M N Sapozhnikov

---

$$i \frac{\partial q}{\partial \xi} = -\frac{1}{2} \frac{\partial^2 q}{\partial \eta^2} - S(\eta)q \left( p + |q|^2 - \mu \frac{\partial |q|^2}{\partial \eta} \right), \quad (1)$$

where  $\eta = x/x_0$  is the normalised transverse coordinate;  $x_0$  is an arbitrary transverse scale;  $\xi = z/L_d$  is the normalised longitudinal coordinate;  $L_d = k_0 x_0^2$  is the diffraction length corresponding to  $x_0$ ;  $k_0 = n_0 \omega/c$  is the wave number;  $n_0$  is the refractive index of the dielectric;  $\omega$  is the central frequency of the radiation spectrum;  $q(\eta, \xi) = A(\eta, \xi)(R_{dr}/I_d)^{1/2}$ ;  $A(\eta, \xi)$  is the complex amplitude of the light field;  $R_{dr} = kL_d/k_0 L_r$ ;  $L_r = 2/kr_{\text{eff}} n^2 E_0$  is the length of nonlinear refraction;  $k = n\omega/c$ ;  $n (\geq n_0)$  is the unperturbed refractive index of the PRC;  $r_{\text{eff}}$  is the effective electrooptical coefficient;  $E_0$  is the static electric field applied to the PRC along the transverse  $x$ -axis;  $I_d$  describes the dark conductivity of the PRC; the parameter  $p = x_0^2(k^2 - k_0^2)/2$  is proportional to the difference of the squares of refractive indices of the dielectric and a photorefractive medium and characterises reflecting properties of the interface; and the parameter  $\mu$  describes the diffusion component of the nonlinear response of the PRC. In fact, equation (1) generalises the known equation from paper [15], which describes the propagation of a laser beam in an infinite PRC.

In (1), the step function

$$S(\eta) = \begin{cases} 1 & \text{for } \eta \in (-\infty, 0), \\ 0 & \text{for } \eta \in [0, +\infty), \end{cases} \quad (2)$$

is also used, which allows one to describe the propagation of a laser beam both in a linear dielectric ( $\eta \geq 0$ ) and a nonlinear photorefractive medium ( $\eta < 0$ ) using one truncated wave equation (1). We assume that the tangential component of the electric field of the light and the normal component of the magnetic induction vector are continuous at the interface  $\eta = 0$ , which, as can be easily shown, corresponds to the continuity of  $q$  and  $\partial q/\partial \eta$ .

The last term in the parentheses in the right-hand side of Eqn (1) describes the beam self-bending caused by energy transfer from low-frequency spatial components of the laser beam to the high-frequency ones. The first term in the parentheses characterises the interaction of the laser beam with the interface between a dielectric and a PRC, while the second term describes the beam self-focusing caused by the drift component of the nonlinear response of a PRC. Finally, the term containing the second derivative over the transverse coordinate  $\eta$  characterises the diffraction spreading of the beam. Inside a linear dielectric (where  $S(\eta) = 0$ ), Eqn (1) transforms to a usual parabolic equation describing diffraction of a light beam in a linear medium. Written in a scalar approximation, this equation can be readily generalised to the case of vector fields taking into account optical activity of a crystal [16]. Note that the propagation of a laser beam in crystals with high optical activity (for example, BSO) can be appreciably affected by the additional modulation of radiation polarisation [17, 18].

Equation (1) was solved numerically using the method of splitting over physical factors. The initial condition at the medium input was specified in the form

$$q(\eta, \xi = 0) = \chi \text{sech}[\chi(\eta - \eta_{\text{in}})],$$

where  $\chi$  is the form factor and  $\eta_{\text{in}}$  is the coordinate of the soliton centre. When parameters  $\mu$  and  $p$  are positive, a

laser beam that entered into a PRC far from the interface will bend toward the interface under the action of the diffusion component of a nonlinear response of the PRC. By approaching the interface between a dielectric and a PRC, the laser beam will experience repulsion from the interface, which can finally result in the total internal reflection from a dielectric medium, which has the lower optical density (see Fig. 1a).

After the first reflection, the beam moves away from the interface and then returns to it because of self-bending. Such consecutive reflections from the interface result in the propagation of the laser beam near the surface. If the angle of incidence is lower than the angle of total internal reflection, the beam is partially refracted to a linear medium and then undergoes the diffraction spreading (see Fig. 1b).

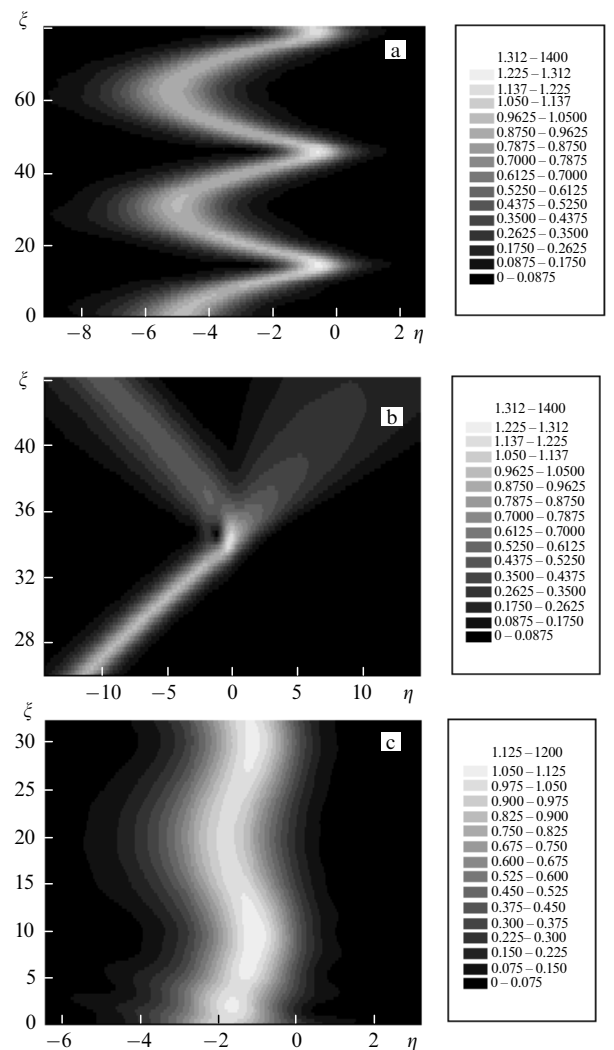


**Figure 1.** Interaction of a laser beam having the hyperbolic secant profile with the interface for  $\mu = 0.1$ ,  $p = 1.0$ ,  $\eta_{\text{in}} = -5.0$  (a),  $-28.0$  (b), and  $-1.81$  (c). The interface is located at the point  $\eta = 0$ .

Another propagation regime is possible when the beam was initially incident close to the interface, so that the reflection dominates over its self-bending. In this case, the beam first moves away from the interface by the distance that is determined by the initial distance from the interface and then it returns to the interface. The most interesting propaga-

tion regime is realised when the repulsion from the interface is completely compensated by the self-bending, resulting in the formation of a stable surface wave (Fig. 1c)

### 3. Profiles of stationary surface waves

We will find the exact profiles of surface modes and study the guiding properties of the interface between a linear dielectric and a PRC. We will seek the stationary localised solutions of equation (1) in the form

$$q(\eta, \xi) = \rho(\eta) \exp(ib\xi),$$

where the envelope  $p \rightarrow 0$  for  $\eta \rightarrow \pm\infty$ . By substituting this expression in (1), we obtain the following second-order ordinary differential equation for the real envelope  $\rho$ :

$$\frac{d^2\rho}{d\eta^2} = 2b\rho - 2S(\eta)\rho \left( p + \rho^2 - 2\mu\rho \frac{d\rho}{d\eta} \right). \quad (3)$$

Equation (3) can be solved numerically by applying the so-called shooting method. This method is based on the fact that inside a linear dielectric ( $\eta > 0$ ) the function  $\rho$  and its derivative  $d\rho/d\eta$  have the following asymptotics, which are valid for  $\eta \rightarrow \infty$ :

$$\rho(\eta > 0) \sim \exp\left[-(2b)^{1/2}\eta\right], \quad (4)$$

$$\frac{d\rho(\eta > 0)}{d\eta} \sim -(2b)^{1/2} \exp\left[-(2b)^{1/2}\eta\right].$$

By specifying the initial conditions in the form (4) in the integration of equation (3) and selecting the corresponding values of parameters  $b$ ,  $p$ , and  $\mu$ , we can obtain localised soliton solutions, whose amplitude  $\rho \rightarrow 0$  for  $\eta \rightarrow \pm\infty$ . To simplify the numerical integration, we approximated the step function  $S(\eta)$ , which describes the properties of the dielectric-PRC interface, by the smoothed function

$$S(\eta) = \frac{1}{2} \left( 1 - \tanh \frac{\eta}{\eta_0} \right), \quad (5)$$

whose form is close to a step. A small parameter  $\eta_0$  in (5) characterises the width of the smoothing region (the typical value  $\eta_0 = 0.05$ ).

Except the convenience of numerical integration, the advantage of this approximation is that it takes into account the spreading of the real interface. By applying the approximation of a narrow intermediate region ( $\eta_0 \ll 1$ ), we can use below (see section 4) the following expression for the derivative of the step function

$$\left( \frac{\partial S}{\partial \eta} \right) \Big|_{\eta_0 \rightarrow 0} = -\delta(\eta), \quad (6)$$

where  $\delta(\eta)$  is the Dirac delta function. In the numerical integration, we varied the propagation constant  $b$  in order to obtain various distributions of the light field, i.e., the surface modes of different orders with asymptotics  $\rho \sim \exp[2(b-p)^{1/2}\eta] \rightarrow 0$  for  $\eta \rightarrow -\infty$ .

Fig. 2 shows profiles of the first three surface modes, which can appear at the dielectric-PRC interface in the

case of a comparatively strong diffusion component of the nonlinear response  $\mu = 0.2$  and the waveguide parameter  $p = 0.5$ . One can see that the wave profiles are asymmetric and their maxima are somewhat shifted to the interface because of the influence of the asymmetric diffusion component of the nonlinear response of the PRC. The width of the intermediate region between a dielectric and a PPC does not virtually affect profiles of surface modes for  $\eta_0 \leq 0.5$ .

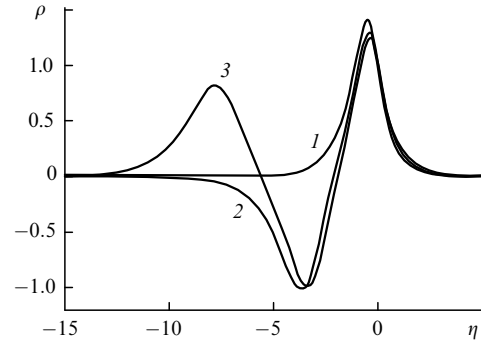


**Figure 2.** Profiles of the first three surface modes at the dielectric-PRC interface for  $\mu = 0.2$ ,  $p = 0.5$ ,  $\eta_0 = 0.05$  and the propagation constants for the first three modes  $b = 1.202$  (1),  $0.904$  (2), and  $0.775$  (3).

As the surface mode order increases, its amplitude decreases and the total power  $P = \int \rho^2(\eta) d\eta$  per unit length along the y-axis increases. As the role of diffusion effects increases (i.e., with increasing parameter  $\mu$ ), the amplitude and the degree of spatial localisation of the surface wave increase. In the limit of purely cubic nonlinearity ( $\mu = 0$ ), localised solutions are absent and surface waves are transformed to periodic, semi-infinite cnoidal waves.

Note that the spatial half-period of the surface wave increases from right to left in fact linearly (Fig. 2). The waveguide parameter  $p$  weakly affects the surface wave profile (we will show below that this parameter noticeably affects only the left wing of the wave) and mainly determines the value of the propagation constant  $b$ . Note that the profile of the first-order surface mode can be well approximated by the known soliton solution in the form of a hyperbolic secant. We will use this fact in the following for the analytic study of the trajectory of a beam with the specified transverse profile near the dielectric-PRC interface.

We also considered the stability of the obtained surface modes using the technique of dispersion diagrams based on the graphical analysis of the dependence of the soliton power on the propagation constant  $b$  [19]. Not presenting here the corresponding diagrams, note that the surface wave power  $P(b)$  is a monotonically increasing function of the propagation constant  $b$ . This suggests that the surface waves in this geometry are stable with respect to small perturbations of input profiles in accordance with the well-known stability criterion  $\partial P / \partial b > 0$  [20].

In addition, we studied the mode stability with the help of a direct computer simulation of the propagation of perturbed surface waves using the method of splitting over physical factors. We considered the effect of substantial (up to 10% in the intensity) harmonic and noise perturbations on the dynamics of propagation of surface waves.

Fig. 3 shows the dynamics of propagation of surface waves of the first and second order in the case of harmonic

perturbation ( $\delta\rho = \delta\rho_0 \cos(\Omega\eta)$ ) of the input profiles. One can see that the perturbation amplitude exhibits oscillations, which decay during the beam propagation. In this case, the energy excess caused by the perturbation of the initial profile passes to the dielectric.

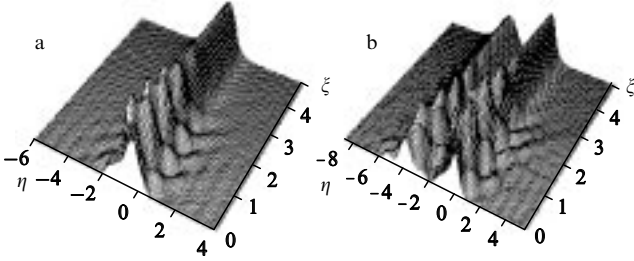


**Figure 3.** Propagation dynamics of surface modes of the first (a) and second (b) orders with perturbed input profiles for the harmonic perturbation amplitude  $\delta\rho_0 = 0.3$  and the perturbation frequency  $\Omega = 4.0$ .

A similar picture was also observed upon excitation of surface modes by beams with profiles close to those of the surface waves. In this case, the energy excess was also rapidly scattered inside the dielectric, and a surface wave of the corresponding amplitude was formed. Note that the stability of the surface waves for a three-dimensional boundary problem was considered in Ref. [21].

We also studied the guiding properties of the dielectric-PRC interface. Fig. 4 shows the dependences of the difference between the propagation constant and the waveguide parameter  $b - p$  on the waveguide parameter  $p$  for the first three surface waves. One can see that there is no cut-off for the higher-order modes and the propagation constant  $b$  is in fact an almost linear function of the waveguide parameter  $p$ .

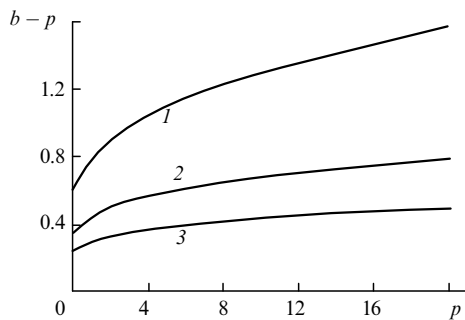


**Figure 4.** Differences  $b - p$  between the propagation constant and the waveguide parameter as functions of the waveguide parameter  $p$  for the first three (1–3) surface modes for  $\mu = 0.2$  and  $\eta_0 = 0.05$ .

An increase in  $p$  results mainly in an increase in the difference between the propagation constants of the modes of different orders and in an increase in the steepness of the left wing of the surface wave (in accordance with the asymptotics  $\rho(\eta \rightarrow -\infty) \sim \exp\{[2(b - p)]^{1/2}\eta\}$ ). One can see from Fig. 4 that the distance between the curves describing the difference between the propagation constant and the waveguide parameter as a function of  $p$  reduces with increasing the mode number. As the mode number  $m$  tends to infinity, the difference between the propagation constant  $b$  and the waveguide parameter  $p$  tends to zero.

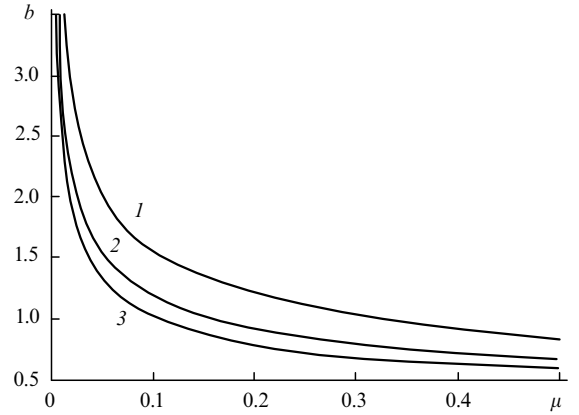


**Figure 5.** Dependences of the propagation constants for the first three (1–3) surface modes on the parameter  $\mu$  for  $p = 0.5$  and  $\eta_0 = 0.05$ .

Fig. 5 shows the propagation constants  $b$  corresponding to fixed modes as functions of the parameter  $\mu$  describing the amplitude of the diffusion component of the nonlinear response of a PRC, the waveguide parameter being specified. One can see that the propagation constant varies within a broad range for the values of  $\mu$  really accessible in experiments.

Note that the propagation constant  $b$  increases infinitely when the parameter  $\mu$  tends to zero, i. e., in passing to a purely cubic nonlinearity. As we mentioned above, the propagation constant  $b$  determines the asymptotics of the right wing of the wave. Therefore, this wing is smoothed with increasing propagation constant. This means in fact that the wave is shifted to the nonlinear medium and is transformed to a nonlinear semi-infinite periodic wave in the limiting case  $\mu = 0$ .

As was mentioned above, the profile of the first surface mode, which can appear at the dielectric-PRC interface, is quite close to a hyperbolic secant. This circumstance allows one, by using the method of effective particles [3], to obtain analytically the equation for the beam trajectory near the interface in the aberration-free approximation, to find the position of the equilibrium point corresponding to the formation of the surface wave, and to determine the depth of the field penetration into a linear dielectric upon reflection.

#### 4. Reflection of a beam from an interface and the surface wave formation

The equilibrium point corresponding to the formation of a surface wave can be readily found by the method of effective particles if the distribution of the light field in a laser beam is known. The method of effective particles is based on a direct analogy between soliton-like objects propagating in a nonlinear medium and quantum-mechanical particles found in a known potential field (in this case, the equilibrium point corresponds to a minimum of the potential energy, provided the latter can be introduced). This method allows one to obtain the trajectory of a particle in the known potential if its localised wave function satisfies equation (1) (the perturbed nonlinear Schrödinger equation) [3].

Using this method, we obtained the ordinary, second-order differential equation

$$w_0 \frac{d^2}{d\xi^2} \eta_c(\xi) = \int_{-\infty}^{\infty} \left[ p \frac{\partial S}{\partial \eta} |q|^2 + \frac{1}{2} \frac{\partial S}{\partial \eta} |q|^4 + \mu S \left( \frac{\partial |q|^2}{\partial \eta} \right)^2 \right] d\eta. \quad (7)$$

for the trajectory of a spatially-localised beam (i.e., a beam under the conditions  $q(\eta \rightarrow \pm\infty, \xi) = 0$  and  $\partial q(\eta \rightarrow \pm\infty, \xi)/\partial \eta = 0$ ) near the dielectric-PRC interface. Here,

$$w_0 = \int_{-\infty}^{\infty} qq^* d\eta$$

is the laser beam power and

$$\eta_c(\xi) = \int_{-\infty}^{\infty} q^* \eta q d\eta / \int_{-\infty}^{\infty} q^* q d\eta \quad (8)$$

is the coordinate of the laser beam centre.

The first term in the integrand in expression (7) describes the influence of reflection from the dielectric-PRC interface on the beam trajectory. The second term characterises the specific self-action of the laser beam in the presence of a guiding surface and, finally, the third term is responsible for the beam self-bending. As the beam is moving away from the interface into the PRC volume (for  $\eta \rightarrow -\infty$ ), the influence of the interface on the beam trajectory weakens and, finally, equation (7) transforms to the equation describing the self-bending of the localised beam in the PRC with the diffusion component of the nonlinear response.

Then, within the framework of the method of effective particles, we assume that the beam self-bending and repulsion from the interface do not distort its initial profile. (The numerical simulation showed that this assumption remains valid even when the reflection from the interface occurs at the angle close to the angle of total internal reflection.) This allows one to obtain the trajectory of the laser beam centre by inserting into the right-hand side of equation (7) the approximate expression for the envelope  $q(\eta, \xi)$  in the form of a hyperbolic secant:  $|q(\eta, \xi)| = \chi \operatorname{sech}\{\chi[\eta - \eta_c(\xi)]\}$  (where  $\chi$  is the form factor), which is a solution of the standard unperturbed Schrödinger equation.

By substituting this solution into equation (7) and taking into account expressions (5) and (6) for the step function  $S$  and its derivative  $\partial S/\partial \eta$ , we obtain the equation

$$\begin{aligned} \frac{\partial^2 \eta_c}{\partial \xi^2} = & -\frac{1}{2}\chi \operatorname{sech}^2(\chi\eta_c) - \frac{1}{4}\chi^3 \operatorname{sech}^4(\chi\eta_c) + \frac{4}{15}\mu\chi^4 \\ & + \frac{2}{5}\mu\chi^4 [\operatorname{sech}^4(\chi\eta_c) - 1] \tanh(\chi\eta_c) + \frac{2}{15}\mu\chi^4 \tanh^3(\chi\eta_c). \end{aligned} \quad (9)$$

which describes the trajectory of the localised beam with the envelope in the form of a hyperbolic secant near the dielectric-PRC interface.

As mentioned above, as the beam is moving away from the interface inside a PRC, i.e., for  $\eta_c \rightarrow -\infty$ , expression (9) transforms to the known equation describing the beam self-bending along the parabolic trajectory

$$\frac{d^2 \eta_c}{d\xi^2} = \frac{8}{15}\mu\chi^4. \quad (10)$$

Equation (9) is analogous to the equation describing the motion of a particle under the action of the nonlinear force  $f(\eta_c)$ . In the absence of energy dissipation, it is convenient to use the potential  $U(\eta_c) = -\int f(\eta_c) d\eta_c$  for a qualitative analysis of possible trajectories of the motion. This potential can be easily calculated and has the form

$$U = -\frac{4}{15}\mu\chi^4 \eta_c - \frac{1}{12}\chi^2 \tanh^3(\chi\eta_c) + \left(\frac{p}{2} + \frac{\chi^2}{4}\right) \tanh(\chi\eta_c)$$

$$\begin{aligned} & + \mu\chi^3 \left\{ \frac{\tanh^2(\chi\eta_c) - 1}{15} + \frac{\operatorname{sech}^4(\chi\eta_c)}{10} + \frac{4 \ln[2 \cosh(\chi\eta_c)]}{15} \right\} \\ & - \frac{p}{2} - \frac{\chi^2}{6}. \end{aligned} \quad (11)$$

The constants in the right-hand side of expression (11) appear due to a convenient normalisation of the potential  $U$  to zero for  $\eta_c \rightarrow \infty$ .

Fig. 6 shows the dependences of the potential  $U$  on  $\eta_c$  for different values of the waveguide parameter  $p$  and different parameters  $\mu$  (hereafter, the form factor  $\chi$  is assumed unity). One can see that the dependence  $U(\eta_c)$  has the form of a potential well of the infinite depth for  $\eta_c \rightarrow -\infty$  and of the zero depth for  $\eta_c \rightarrow \infty$ . This suggests that both the finite periodic and infinite motions can take place. The slope of the left wing of the potential well increases linearly with increasing parameter  $\mu$  (see Fig. 6b).

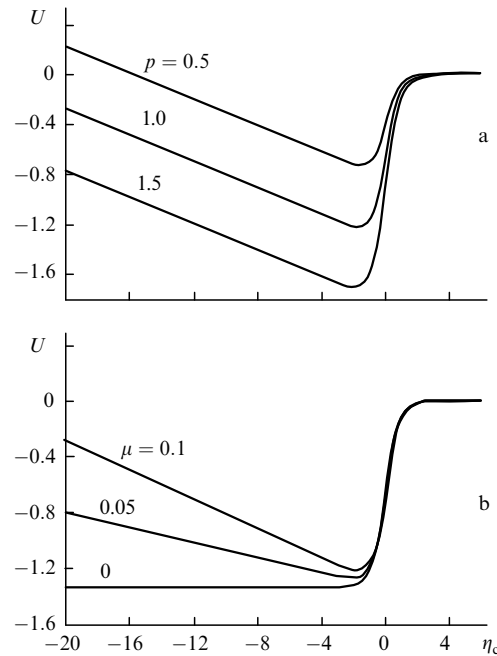


**Figure 6.** Form of the potential  $U(\eta_c)$  for a PRC for  $\eta_0 = 0.05$ ,  $\mu = 0.1$  and different values of  $p$  (a) and  $p = 1.0$  and different values of  $\mu$  (b).

When  $\mu$  is zero, the potential has the form of a step, i.e., finite motions are impossible in this case. The waveguide parameter  $p$  determines the depth of the potential well, which increases with increasing  $p$  (Fig. 6a). The minimum of the potential energy corresponds to the stable equilibrium point, which is characterised by an exact energy balance between the beam self-bending and repulsion from the dielectric-PRC interface. Thus, for  $\mu = 0.1$ ,  $p = 1.0$ , and  $\chi = 1.0$ , the equilibrium point is located approximately at  $\eta_{in} = -1.81$ .

Fig. 1c shows the dynamics of propagation of the laser beam with a profile described by a hyperbolic secant. The beam was introduced into a nonlinear photorefractive medium at the point  $\eta = \eta_{in}$  [Fig. 1c presents the results of numerical integration of the truncated wave equation (1)]. One can see that the beam centre coordinate weakly oscillates in the transverse direction during the beam propagation. This is caused mainly by the transformation of the initial secant

envelope to a slightly asymmetric profile of the first surface mode.

The trajectories of the beam propagation calculated for different initial distances  $\eta_{in}$  using equation (9) well agree with the results of a direct numerical integration of the initial truncated wave equation (1).

The potential (11) also allows one to estimate the critical distance  $\eta_{cr}$  of the beam penetration into a nonlinear medium. A laser beam incident on a PRC at the point separated from the interface by the distance above  $\eta_{cr}$  will refract into a linear dielectric. The critical distance  $\eta_{cr}$  can be found from the relation  $U(\eta_{cr}) = 0$ , which determines the boundary between the regions of finite [ $U(\eta_c) < 0$ ] and infinite [ $U(\eta_c) > 0$ ] types of the motion. Taking into account that for large negative values of  $\eta_c$ , the function  $\tanh(\chi\eta_c) \rightarrow -1$  and  $\text{sech}(\chi\eta_c) \rightarrow 0$ , we can obtain the simple expression for the critical distance:

$$\eta_{cr} = -\frac{15p + 5\chi^2}{8\mu\chi^4}. \quad (12)$$

The turning points corresponding to the finite motion (i. e., in fact the depth of penetration of the laser beam inside a linear dielectric or the minimal distance to which the beam centre approaches the interface) can be readily found graphically from the form of the potential  $U$ , which is clearly seen from the first integral of equation (9)

$$(d\eta_c/d\xi)^2 = 2U(\eta_{in}) - 2U(\eta_c), \quad (13)$$

where  $\eta_{in}$  is the coordinate of the point of entry of the laser beam centre into a nonlinear medium. The turning points can be determined from the condition  $d\eta_c/d\xi = 0$ , i. e., knowing  $\eta_{in}$ , we can find the second turning point from the condition  $U(\eta_c) = U(\eta_{in})$ .

One can see from Fig. 6 that the right wing of the potential well near the point  $\eta_c = 0$  also can be approximated by a linear function. This circumstance allows us to derive the following relation between the positions of the right and left turning points lying on linear parts of the potential  $U$ :

$$\begin{aligned} & \left( \frac{1}{2}p\chi + \frac{1}{4}\chi^3 - \frac{4}{15}\mu\chi^4 \right) \eta_{right} \\ &= \frac{3}{2}p + \frac{1}{2}\chi^2 - \frac{1}{3}\mu\chi^3 - \frac{4}{15}\chi^3 \ln 2 + \frac{8}{15}\mu\chi^4 \eta_{left}. \end{aligned} \quad (14)$$

In conclusion, note that the method of effective particles is well applied to the beams with the envelope that is close to the envelope of the first surface mode. However, the application of this method to higher-order modes involves certain difficulties because of the lack of even approximate analytic expressions for the mode envelopes.

## References

1. Tomlinson W, Gordon J, Smith P, Kaplan A *Appl. Optics* **21** 2041 (1982)
2. Akhmediev N N, Korneev V I, Kuz'menko Yu V *Zh. Eksp. Teor. Fiz.* **88** 107 (1985)
3. Newell A, Moloney J *Nonlinear Optics* (Redwood City: Addison-Wesley, 1992)
4. Tran H J. *Nonlin. Opt. Phys. Mater.* **5** 133 (1996)
5. Powell J, Wright E, Moloney J J. *Appl. Math.* **54** 774 (1994)

6. Duree G, Shultz J, Salamo G, Segev M, Yariv A, Crisignani B, Di Porto P, Sharp E, Neurgaonkar R *Phys. Rev. Lett.* **71** 533 (1993)
7. Iturbe-Castillo M, Marquez-Aguilar P, Sanchez-Mondragon J, Stepanov S, Vysloukh V *Appl. Phys. Lett.* **64** 408 (1994)
8. Garcia-Quirino G, Sanchez-Mondragon J, Stepanov S *Phys. Rev. A* **51** 1571 (1995)
9. Cronin-Golomb M *Opt. Lett.* **20** 2075 (1995)
10. Garcia-Quirino G, Sanchez-Mondragon J, Stepanov S, Vysloukh V *J. Opt. Soc. Am. B: Opt. Phys.* **13** 2530 (1996)
11. Christodoulides D, Coskin T *Opt. Lett.* **21** 1220 (1996)
12. Raita E, Kamshilin A, Jaaskelainen T J. *Opt. Soc. Am. B: Opt. Phys.* **15** 2023 (1998)
13. Kamshilin A, Raita E, Khomenko A J. *Opt. Soc. Am. B: Opt. Phys.* **13** 2536 (1996)
14. Kutuzov V, Petnikova V, Shuvalov V, Vysloukh V J. *Nonlin. Opt. Phys. Mater.* **6** 421 (1997)
15. Christodoulides D, Carvalho M J. *Opt. Soc. Am. B: Opt. Phys.* **12** 1628 (1995)
16. Singh S, Christodoulides D J. *Opt. Soc. Am. B: Opt. Phys.* **13** 719 (1996)
17. Fuentes-Hernandez C, Khomenko A *Phys. Rev. Lett.* **83** 1143 (1999)
18. Kamshilin A, Paivasaari K, Khomenko A, Fuentes-Hernandez C *Opt. Lett.* **24** 832 (1999)
19. Snyder A, Mitchell D, Kivshar Y *Mod. Phys. Lett. B* **9** 1479 (1995)
20. Mitchell D, Snyder A J. *Opt. Soc. Am. B: Opt. Phys.* **10** 1572 (1993)
21. Vysotkina N N, Rozanov N N, Smirnov V A *Zh. Tekh. Fiz.* **57** 173 (1987)